Controlling Micellar Structure of Amphiphilic Charged Triblock Copolymers in Dilute Solution via Coassembly with Organic Counterions of Different Spacer Lengths

Honggang Cui,[†] Zhiyun Chen,[‡] Karen L. Wooley,*[,‡] and Darrin J. Pochan*[,†]

Department of Materials Science and Engineering and Delaware Biotechnology Institute, University of Delaware, Newark, Delaware 19716, and Center for Materials Innovation and Department of Chemistry, Washington University in Saint Louis, Saint Louis, Missouri 63130

Received April 21, 2006; Revised Manuscript Received July 7, 2006

ABSTRACT: Micelle structures from the assembly of poly(acrylic acid)-*block*-poly(methyl acrylate)-*block*-polystyrene (PAA-*b*-PMA-*b*-PS) triblock copolymers in mixed tetrahydrofuran (THF)/water solution, including disks, toroids, cylinders, and spheres, were targeted by coassembling with different diamines. At constant solution composition (THF:H_2O, polymer concentration, and diamine concentration), the interfacial curvature of the assembled structures was determined primarily by diamine chain structure. It was found that interchain binding from the interaction of the two amine end groups of diamines with acid groups from different PAA corona blocks governs the final assembled structures. Diamines with hydrophilic spacers induced the formation of micelles with larger interfacial curvature as the spacer length increased. Disklike micelles, cylindrical micelles, or spherical micelles were observed with the gradual increase of hydrophilic spacer length. Diamines with variable hydrophobic spacers showed a similar effect when the spacer length was less than six methylene units. Application of longer hydrophobic diamines had a reverse effect on the interfacial curvature. This effect was attributed to the interaction of hydrophobic diamine hydrocarbon linking chains with the PMA-*b*-PS hydrophobic core. These findings indicate an easy method to tune micelle structure with multivalent organic counterions. Assembled morphologies were characterized by means of transmission electron microscopy, and the interaction of diamines with acidic units of the PAA block segments was studied by solution-state nuclear magnetic resonance spectroscopy.

Introduction

Controlling the assembled structure of amphiphiles is of great practical value and has received tremendous interest due to current and potential applications in the fields of materials science,[1−5] bioengineering,[6,7] and the pharmaceutical industry.[8,9] The associative behavior and aggregate structure of small molecular amphiphiles, such as surfactants and lipids, are fairly well understood experimentally and theoretically.[10] The packing geometry in surfactant systems is tunable by adjusting the molecular structure, surfactant concentration, solvent properties, and temperature.[11] Recently, amphiphilic block copolymers, the macromolecular analogues of conventional surfactants, have been recognized for advantages such as low critical micelle concentration (cmc), more robust assemblies, highly tunable composition and chain architecture, micellization depending on selective solvents, and abilities to trap unstable or metastable structure due to slow kinetics.[12,13] The combination of these different features offers great flexibility for developing novel assembled morphologies and outstanding ability to control and manipulate those morphologies. A variety of morphologies originating from the solution-state self-assembly of amphiphilic copolymers, which are rarely observed in surfactant systems, have been discovered including toroids,[14] helices,[15] nanotubes,[16] disks,[17,18] hollow hoops,[19] and nanospheres.[20] Notably, when charged blocks were introduced in replacement of neutral hydrophilic blocks, assembled structures could be manipulated through ion−ion interaction by adding external counterions.[14,15,20]

Therefore, by taking advantage of the design flexibility of block copolymer/solvent systems, one can produce assembled structures in a controlled way. Three main strategies have been pursued to control the block copolymer supramolecular assembly process with the aim of obtaining highly tailored materials:[21] (1) choice of block copolymer molecules, (2) selectivity of added solvents, and (3) application of solution stimuli. The first important design parameter is the molecular level structure of block polymers themselves, including the types of blocks, chain length of different blocks, and chain architecture.[14,22−26] Second, the micelle structure is tunable by choosing different solvents that are selective to one or more blocks.[27−33] Eisenberg's group[29−31] proposed that not only could aggregation morphology be controlled by the solvent properties, but also the aggregate size is controllable by changing the relative ratio of different solvents. Third, the application of solution stimuli presents a route for both control of aggregate morphology and size and the potential control of material function. Examples of external stimuli studied are acids,[34,35] bases,[35] salts,[34−36] or surfactants.[37−48] Zhang et al.[34] initially reported that the addition of ions can change morphology of "crew-cut" aggregates of polystyrene-*b*-poly(acrylic acid) copolymers in dilute solution. More recently, Förster and co-workers[36] proposed that charged diblock copolymer micelles fused into toroidal networks in the presence of a higher concentration of salts in aqueous solution. Effort has also been devoted to studying complex micelle formation from coassembly of nonionic block copolymers with surfactants.[37−43] Multiple morphologies other than spheres have also been reported from mixed systems of ionic copolymers with surfactants.[44−48] Among the three block copolymer supramolecular assembly strategies, changing solvent properties and addition of counterions are most convenient experimentally

[†] University of Delaware.
[‡] Washington University in Saint Louis.
* Corresponding authors. E-mail: klwooley@artsci.wustl.edu; pochan@udel.edu.

10.1021/ma0609026 CCC: $33.50
Published on Web 08/18/2006

because new block copolymers demand new laborious synthetic efforts. In this context, we are taking advantage of all three design parameters, particularly the addition of counterions, to control the structural features of final assembled micelles. Our system consists of (1) a designed linear triblock copolymer with a chargeable hydrophilic PAA block connected sequentially to PMA and then PS hydrophobic blocks, (2) mixed THF and water solvents with variable ratios, and, most importantly, (3) application of diamino organic counterions with different chain structures.

It has been shown that the addition of inorganic salts will cause charged micelle corona to shrink and the aggregation number to increase in an equilibrium system because of electrostatic screening of repulsions between chains. These effects can, to some extent, change the assembled micelle morphology.[35,49−52] Literature examples show that multivalent salts demonstrated greater ability to modify assembled structures compared to monovalent inorganic salts.[53] However, the use of inorganic counterions to control aggregate structure seems to be limited to a narrow range of relative block compositions. For example, block copolymers with a long hydrophilic block did not produce morphologies other than spherical micelles, even with addition of a considerable amount of inorganic salt.[29] In comparison to inorganic salts, organic counterions can afford enormous advantages in manipulating the block copolymer assembly structure via the widely adjustable organic counterion properties of chain hydrophobicity, chain architecture, valence, and volume as well as the selectivity to solvents. However, the interactions of amphiphilic copolymers with organic counterions, especially counterions with long hydrocarbon chains, are more complicated than with inorganic salts. The addition of multivalent organic counterions into charged micelle systems could not only screen the electrostatic repulsions in the corona but also bridge separate chains together by forming either hydrogen bonds or compact ion pairs. Primarily, to date, the interaction behavior of inorganic salts with charged polymer micelles or brushes has been studied. To the best of our knowledge, the effect of molecular structure of organic counterion on assembled structure of amphiphilic, polyelectrolyte-containing block copolymers has not yet been studied systemically. This paper is devoted to determining conditions under which the micellar structure of PAA-*b*-PMA-*b*-PS copolymer can be controlled in THF/H_2O solutions by choosing organic diamines of different chain structures.

Experimental Section

Materials. The triblock copolymer poly(*tert*-butyl acrylate)-*block*-poly(methyl acrylate)-*block*-polystyrene (P*t*BA-*b*-PMA-*b*-PS) was synthesized by sequentially incorporating *tert*-butyl acrylate (*t*BA), methyl acrylate (MA), and styrene (S) through an atom transfer radical polymerization (ATRP) procedure.[14,54] The *tert*-butyl esters of P*t*BA-*b*-PMA-*b*-PS were selectively cleaved via reaction with iodotrimethylsilane (Me3SiI) in dichloromethane, giving the amphiphilic block copolymer poly(acrylic acid)-*block*-poly(methyl acrylate)-*block*-polystyrene (PAA_{99}-*b*-PMA_{73}-*b*-PS_{66}; M_w: 2.04×10^5 Da; M_w/M_n: 1.05).[14] After removal of all the solvent and excess reagent, the resulting polymer solid was dissolved in THF, decolored by 1% $Na_2S_2O_5$ aqueous solution, and purified by extensive dialysis against Nanopure water. Organic diamines, with the exception of 1,2-di(2′-(2″-aminoethoxyl)-ethoxyl)ethane (PEG5 diamine), were purchased from Sigma-Aldrich and used as received (Table 1). PEG5 diamine was synthesized by a modified method.[55,56]

The sample solutions were prepared by dissolving the triblock copolymer into THF with a specific amount of organic counterion. The ratio of amine groups from organic counterions to acid groups from PAA blocks was fixed as 1:1. The mixture was stirred rigorously overnight to ensure complete dissolution of copolymer. Then a certain amount of Milli-Q deionized water was introduced into the solution. The initial concentration of copolymer in solution was 0.1 wt % in THF before adding water and consequently decreased with the introduction of water. Control experiments showed that the change of block copolymer concentration in this range (0.1−0.02 wt %) did not induce any difference in assembled polymer structure.

Table 1. Structure of Diamines Used in This Study

diamine	structure
DI2	$H_2NCH_2CH_2NH_2$
DI4	$H_2N(CH_2CH_2)_2NH_2$
DI6	$H_2N(CH_2CH_2)_3NH_2$
DI8	$H_2N(CH_2CH_2)_4NH_2$
EDDA	$H_2N(CH_2CH_2O)_2CH_2CH_2NH_2$
PEG5	$H_2N(CH_2CH_2O)_4CH_2CH_2NH_2$

Transmission Electron Microscopy. TEM experiments were performed on a JEOL 2000FX microscope operating at an accelerating voltage of 200 kV. TEM samples were prepared by applying a drop of polymer solution (about 2 μL) directly onto a carbon-coated copper TEM grid and allowing the solution to evaporate under ambient conditions. Afterward, a droplet of freshly made, saturated uranyl acetate aqueous solution (about 10 μL) was deposited onto the dried samples. After ca. 3 min, the excess solution was wicked away by a piece of filter paper. The sample was then allowed to dry under ambient conditions. In-situ cryo-TEM imaging has shown micelle structures with the same packing geometry as those in cast films, indicating that micelle structure in cast films reflected in-situ micelle solution structures.

Results and Discussion

1. Effect of Diamines with Different Hydrophilic Chain Length on Assembled Structures. Generally speaking, when organic diamines were added, structures with different interfacial curvature could be developed depending on counterion type and amount. Without diamine addition, PAA_{99}-*b*-PMA_{73}-*b*-PS_{66} copolymers are not able to assemble into any structures other than spherical micelles at all THF:water solution ratios due to repulsions between charged PAA corona chains causing significant interfacial curvature toward the THF-swollen PMA-*b*-PS. Under the same solution conditions, hydrophilic diamines with different spacer length induced the formation of morphologies different from spherical micelles. Figure 1A−C shows typical TEM images obtained from three different hydrophilic diamines with different spacer length between the two amine end groups. Ethylenediamine induced the formation of disklike micelles (Figure 1A) while 2,2′-(ethylenedioxy)bis(ethylamine) (EDDA), with longer hydrophilic spacer length, induced cylindrical micelle formation (Figure 1B). PEG5 diamine, which has double the chain spacer length of EDDA, formed spherical micelles (Figure 1C).

The major forces governing self-assembly of neutral amphiphilic copolymers are a balance of three contributions: an interfacial free energy and two penalty terms from chain stretching of grafted hydrophilic corona and hydrophobic core blocks.[57] Chain stretching in the corona is due to the short-range, interunit repulsive interaction because of high grafting density. In a charged micelle system, this chain stretching is a combination of short-range, nonelectrostatic interactions with long-range electrostatic force but is dominated primarily by electrostatic interactions.[58] Hence, because the strength of electrostatic interactions in the corona can be manipulated through the ion−ion interactions, the final morphology is tunable by adding external counterions. Multivalent salts present in the polyelectrolyte micelle solution can either neutralize charges

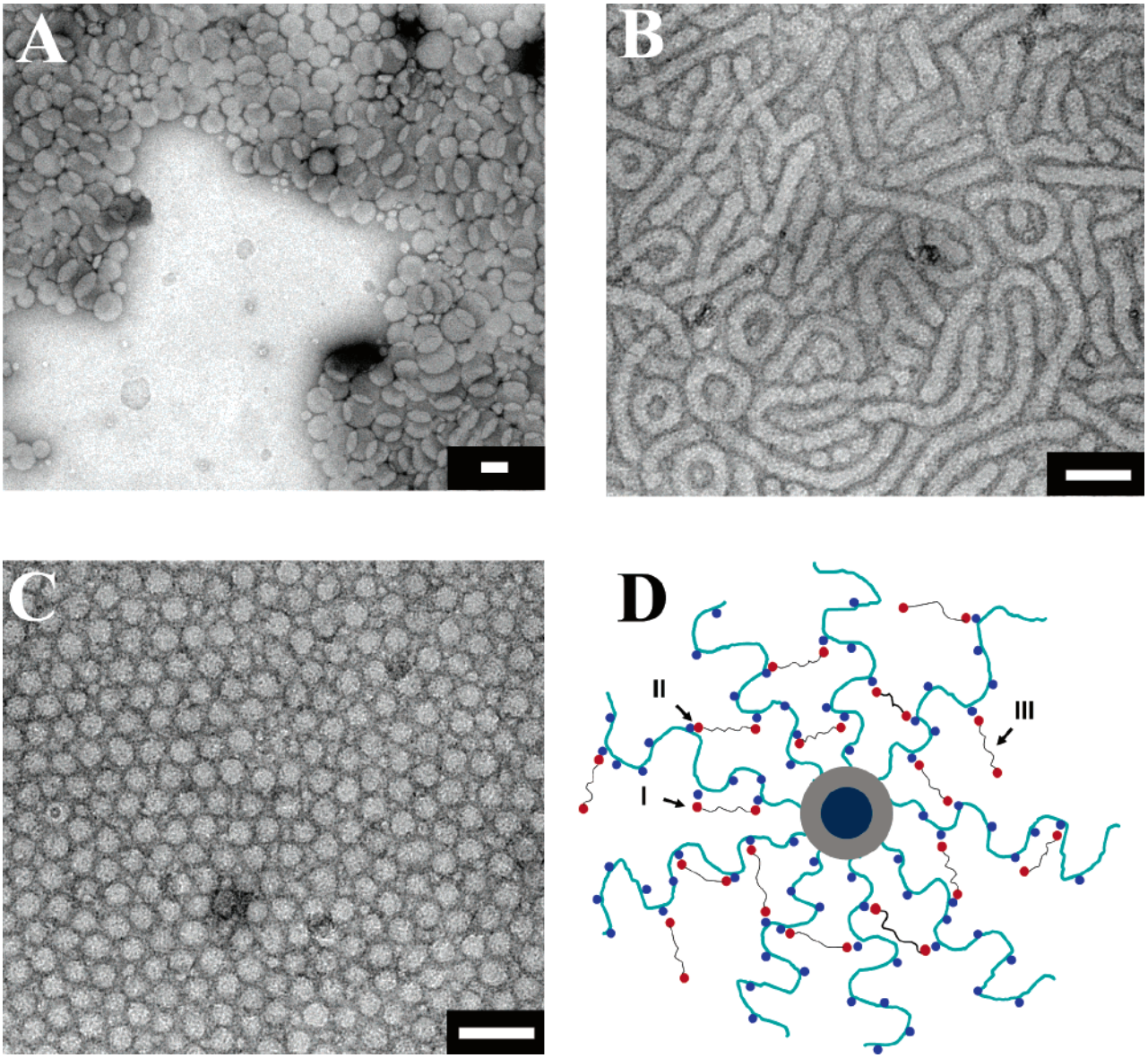

Figure 1. Micelle structure strongly depends on the diamine hydrophilic spacer length. The ratio of THF to water was 1:2, and the molar ratio of amine group to acid group was fixed as 1:1. (A) Disklike micelles, ethylenediamine; (B) cylindrical micelles, EDDA; (C) spherical micelles, PEG5; (D) schematic showing the three ways that diamines may interact with PAA blocks: (I) intrachain bonding; (II) interchain bonding; (III) only one end of diamine bonding with PAA chain. Scale bar: 100 nm.

on the polymer chains in the corona via complexation or screen electrostatic interactions if trapped in the corona.[52] Both complexation and screening would weaken the electrostatic interaction between polymer chains in the corona so as to make the block behave more like nonionic amphiphiles. However, the introduction of the same molar concentration of organic counterions but with different controllable chain structure provides micelle geometry control, indicating that electrostatic interactions in and of themselves are not the reason for micelle geometry manipulation.

In fact, interchain binding of diamines with different PAA chains is mainly responsible for modifying the interfacial curvature of assembled structures. When water was added into the copolymer/THF solution, it was preferentially distributed around PAA chains.[53] Since the diamine backbones are hydrophilic, it is reasonable to assume that hydrophilic diamines prefer to interact with PAA in the micelle corona. Once organic diamines are trapped in the corona, they can interact with PAA acidic units in three ways (Figure 1D): bonding with two acrylic acid units from two different PAA chains (interchain binding) or from the same PAA chain (intrachain binding) or only binding with one acrylic acid retaining one free amine in the corona. Only these diamines that produce interchain binding can bring repulsed chains together and have a significant effect on corona packing, chain conformation, and consequent interfacial curvature to change the micelle geometry. Because of the interchain binding, the distance of these two PAA chains in the corona would be closely related to the spacer length between two amine groups. The shorter the diamine spacer length, the closer the PAA can be crowded. Indeed, the interfacial curvature of assembled structure is a result of a gradual change of spacer length. The bridging effect of diamines was further tested by using a hydrophilic monoamine, 2-methoxyethylamine. Under the same solution conditions as in Figure 1, PAA_{99}-*b*-PMA_{73}-*b*-PS_{66} copolymers only formed spherical micelles in the presence of monoamine.[14] Monoamine is incapable of binding two different chains and only provides electrostatic screening of the corona PAA chains.

The effects of organic counterion molecular structure, including multivalency and chain architecture, have also been studied

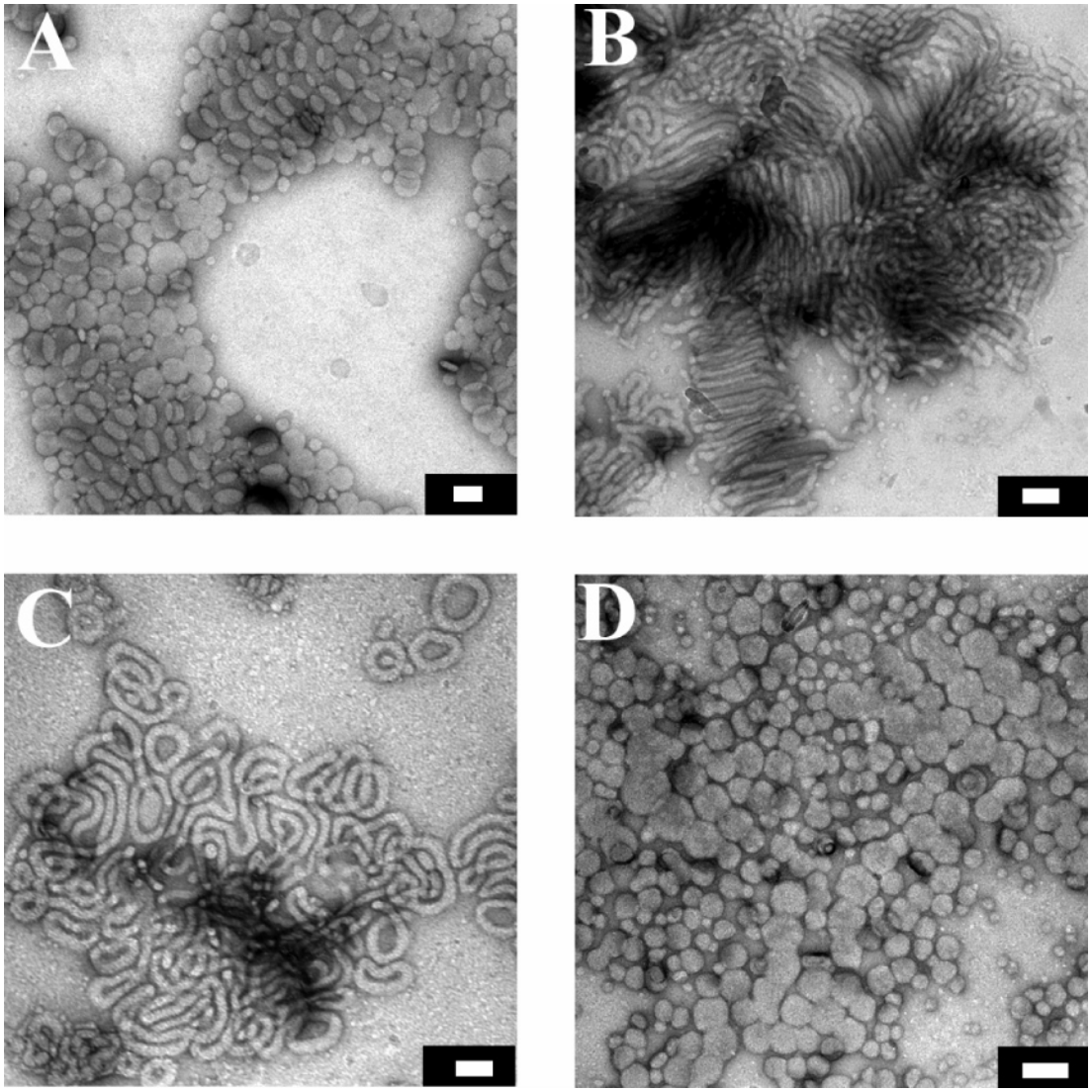

Figure 2. Morphologies with distinct local interfacial curvature via coassembly with diamines of different hydrophobic spacer lengths. The ratio of THF to water was 1:2, and the ratio of amine group to acid group was fixed as 1:1. (A) Disklike micelles with DI2; (B) cylindrical micelles with DI4; (C) cylindrical micelles with DI6; (D) disklike micelles with DI8. Scale bar: 100 nm.

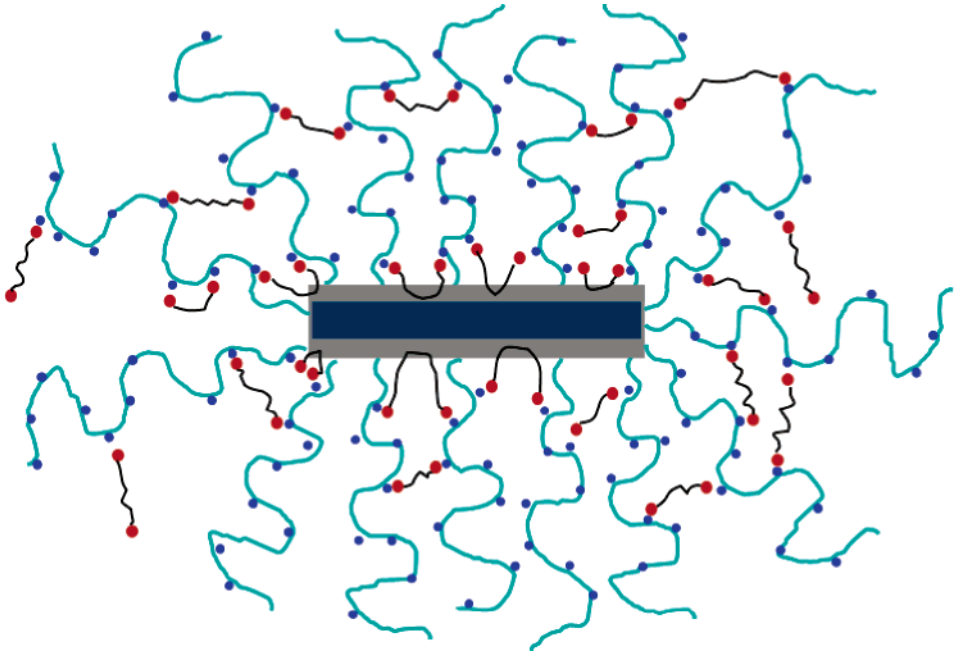

Figure 3. Schematic showing the interaction between triblock copolymer and diamines with longer hydrophobic spacer length; diamine can also promote morphological change by dipping into hydrophobic cores in addition to bonding with separate PAA chains in corona.

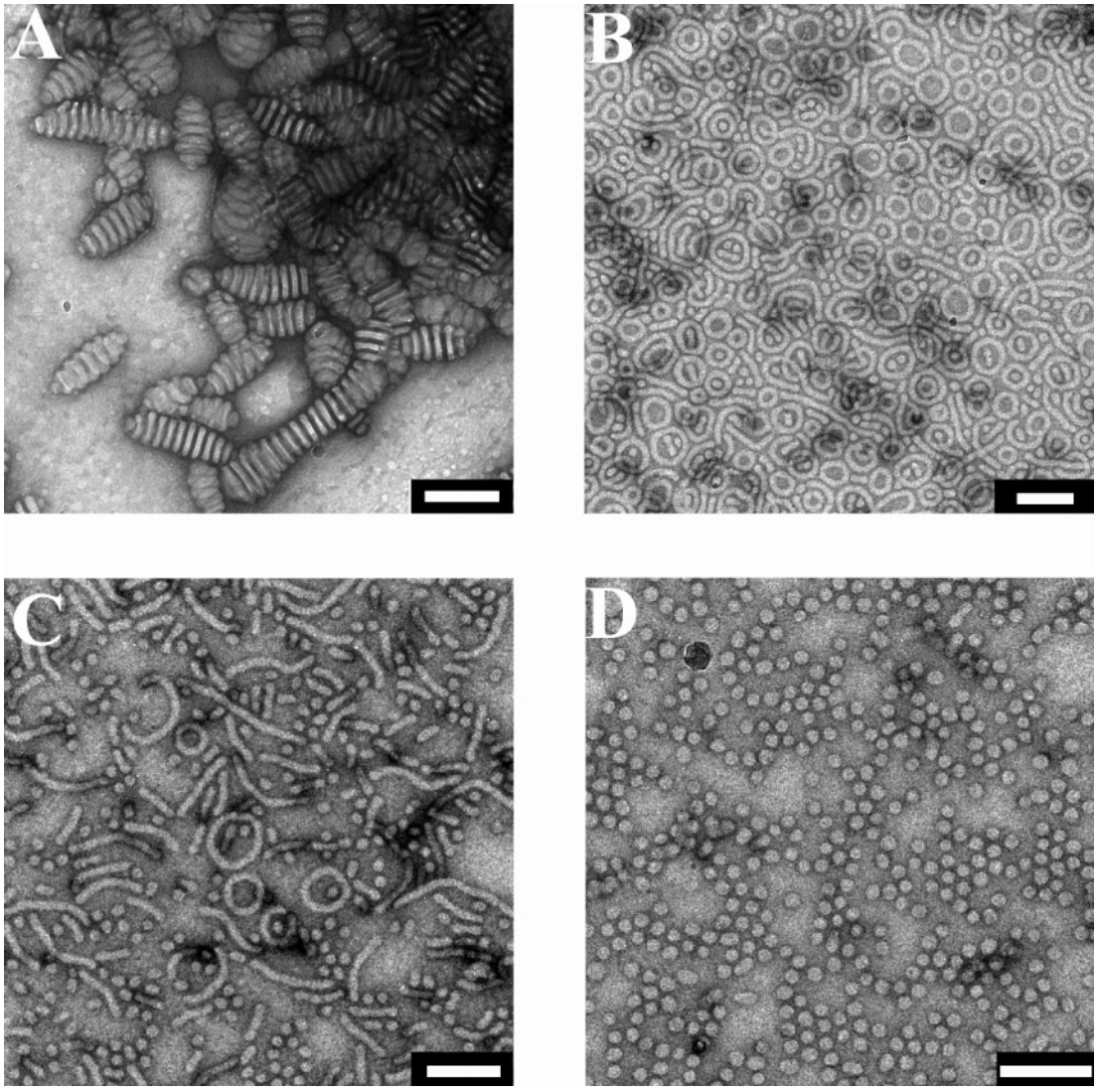

Figure 4. Assembled morphologies of PAA_{99}-*b*-PMA_{73}-*b*-PS_{66} in THF/water solution in the presence of EDDA. The copolymer and EDDA were dissolved in THF. The ratio of amine group to acid group was 1:1. Then water was titrated into the solution at the rate of 0.6 wt %/min. Different morphologies were observed depending on the ratio of THF to water. (A) Packed bilayer structure, THF:water = 2:1; (B) predominantly toroidal micelles, THF:water = 1:2; (C) mixed cylindrical micelles with spherical micelles, THF:water = 1:3; (D) spherical micelles, THF:water = 1:4. Scale bar: 200 nm.

in DNA/polycation complex systems. It was reported that the arrangement of DNA strands in complexes is determined by the structure of the polycation.[59−61] Schellman et al. reported that collapsed DNA helices could form a hexagonal array with organic counterions in the interstices between helices. The Bragg spacing for this collapsed DNA structure was dependent on the adjustable spacer length of the methylene bridge between two adjacent amine groups based on X-ray diffraction studies.[61]

Another reason for the formation of different micelles may arise from the volume occupied by the different spacers. To minimize the PAA-*b*-PMA interfacial area, one can imagine that copolymer chains through the interface must be crowded. It is unfavorable for organic counterions with larger volume (longer spacer) to inhabit a corona interior. Any diamines deep in the corona can complex with acid groups close to the hydrophilic/hydrophobic interface and would strongly contribute to the morphology transition. As a result, PEG5 diamine with the longest spacer will be squeezed out of the interfacial region. In contrast, ethylenediamine, due to its smaller molecular volume, has more opportunity to interact with acids closer to the PAA-*b*-PMA interface. In either case, it can be concluded that diamines with shorter hydrophilic spacer length more significantly affect interfacial curvature and, thus, micelle structure.

2. Effect of Diamines with Different Hydrophobic Chain Length on Assembled Structures. When diamines with hydrophobic chain linkers were employed, the dependence of micelle geometry on linker length observed for shorter hydrophobic linkers was similar to that observed with hydrophilic diamines. Figure 2A again shows the dominant disklike structure induced by ethylenediamine (image taken from the same sample as Figure 1A). With the increase of spacer length from two to six methylene groups (Figure 2A−C), the morphologies vary from disks to cylinders. Spacer length dependence is the same as had been observed for hydrophilic diamines. Interestingly, when diamine spacer length was increased to eight methylene units, the morphology reverted to a disk structure rather than spherical as was observed with hydrophilic spacers in Figure 2D.

The hydrophobic diamines seem to behave as amphiphiles themselves. The interactions between the amphiphilic diamines and the block copolymer are not limited to electrostatic screening and inter-acid bonding in the corona. With the increase of hydrocarbon chain length, diamine counterions have more

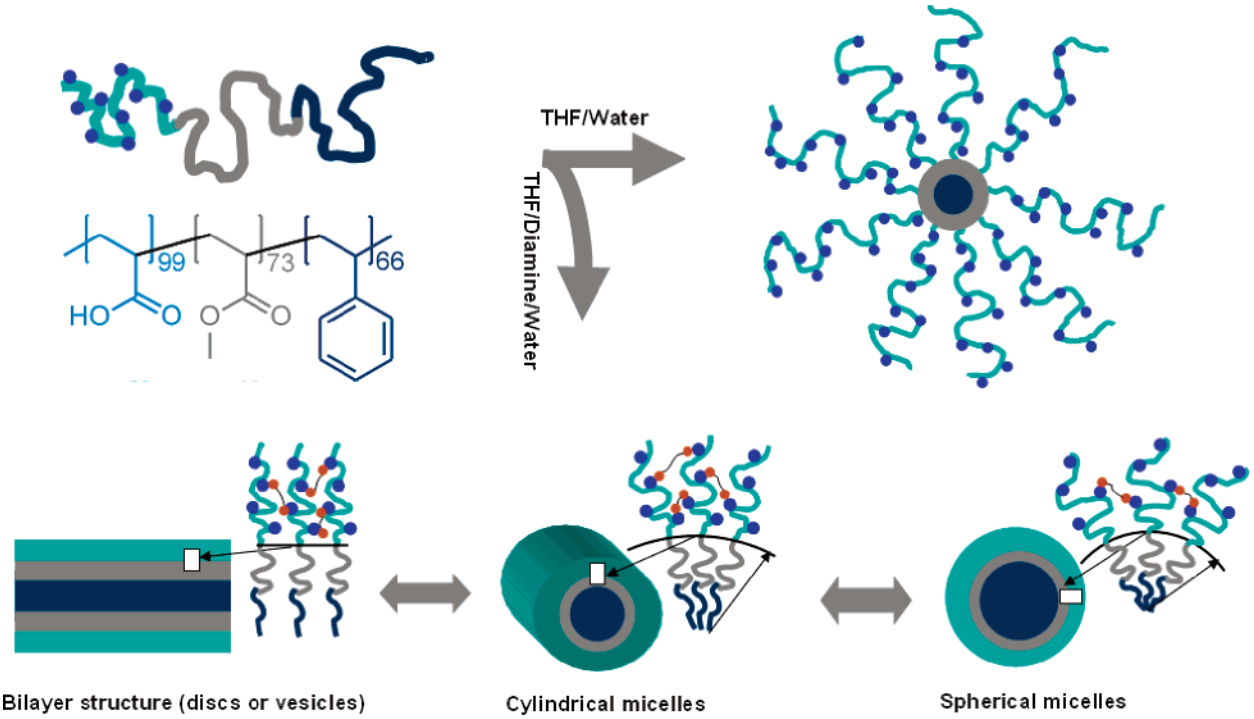

Figure 5. Schematic of micelle formation of PAA_{99}-*b*-PMA_{73}-*b*-PS_{66} in THF/water solution. Without any diamine in solution, the block copolymer only associates into spherical micelles. In the presence of diamines, morphologies other than spherical micelles, such as bilayer structured micelles or cylindrical micelles, can be formed depending on diamine chain structure. With a certain amount of specific diamine, the morphology is also tunable by varying the mixed ratio of THF to water. With the increase of water content, amphiphilic block copolymer tends to form micelles with higher interfacial curvature.

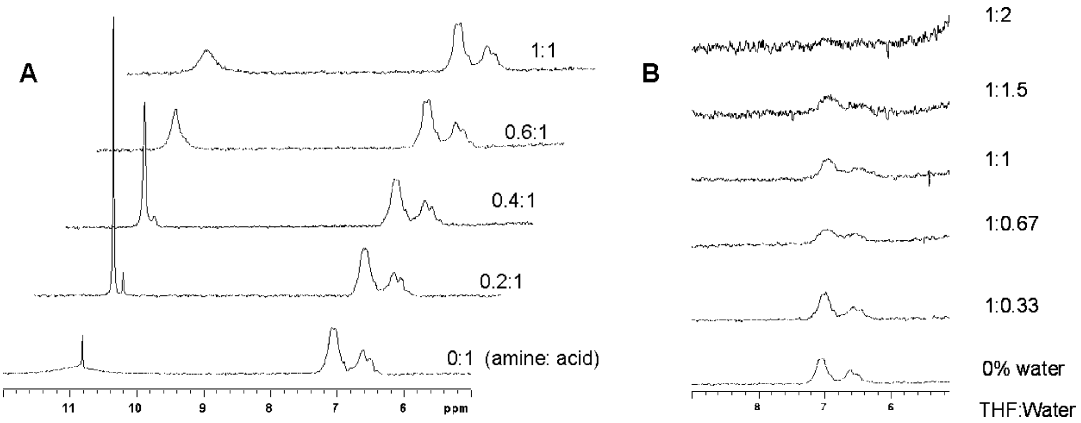

Figure 6. (A) NMR spectra of PAA_{99}-*b*-PMA_{73}-*b*-PS_{66} in THF-d_8 solution with titration of different amounts of diamine (EDDA). The ratios of amine groups to acid groups are given in the plot. The spectra were shifted for clarity. (B) NMR spectra of PAA_{99}-*b*-PMA_{73}-*b*-PS_{66} in THF-d_8/EDDA solution (amine:acid = 1:1) with progressive addition of water. The ratios of THF to water are given on the right of the plot.

tendency to interact with the PS-*b*-PMA blocks in the hydrophobic core. The hydrophobic linker could associate with the hydrophobic core while charged headgroups remain in the corona (Figure 3). A hairpin structure could be formed for diamines with long enough hydrophobic spacers by which the two amine ends remain within the PAA corona while the hydrophobic spacers extend into the PMA-*b*-PS core. The bending energy penalty for forming this hairpin structure is too high for short-chain diamines but becomes less significant relative to interactions for diamines having more than six methylene units. It is hypothesized that once this hairpin structure is formed, some diamines act as spacers across the interface, causing a decrease of interfacial area per copolymer chain that favors micelle structures with lower curvature. Moreover, hydrophobic linkers of diamine add volume into the closely packed hydrophobic core that, in turn, induces further stretching of the PMA-*b*-PS chains, also leading to the formation of micelles with lower interfacial curvature. Additionally, electrostatic repulsive interactions between charged chains close to the interface are reduced significantly due to the formation of diamine hairpin structure because the charged PAA blocks close to the interface are neutralized due to the interaction with amine groups from the diamines placed into hydrophobic core. In summary, the longer the hydrophobic chain between two amine groups, the more likely the hydrocarbon linkers will partition into the hydrophobic core. If PAA-amine binding and hydrophobic interaction coexist, the amphiphilic copolymer tends to form micelles with lower curvature due to the increase of hydrophobic spacer length.

3. Effect of the Ratio of THF to Water on Assembled Structures. Using mixed solvents is a standard technique to produce different assembled structures for amphiphilic block copolymers.[14,25,62] In these studies, it was found that different morphologies could be formed depending on the amount of

water titrated into the THF/polymer/diamine system. A range of morphologies is possible with water titration using PAA_{99}-*b*-PMA_{73}-*b*-PS_{66} block copolymer in the presence of EDDA organic counterions at a ratio of amine to acid groups of 1:1. Figure 4 shows different morphologies assembled with different ratios of THF to water. The morphologies range from a closely packed bilayer structure, to toroidal/cylindrical micelles, and to spherical micelles. It can be seen that as the water content was increased the interfacial curvature between the hydrophilic and hydrophobic blocks increased. The increase of interfacial curvature can be generally attributed to the shrinking of the volume occupied by the PS-*b*-PMA hydrophobic blocks and increasing expansion of the PAA corona with the progressive addition of water. It is worth mentioning that the structure shown in Figure 4A is very similar to the lamellar phase usually observed in bulk phase separation of block copolymers. Bulk phase separation of the solution in Figure 4A occurred after sitting quiescently for several days, suggesting that these closely packed bilayer structures might be bulk-phase-separated, polymer-rich droplets, highly swollen by solvents, and exhibiting bulklike, lamellar nanostructure. A detailed discussion of these phase-separated droplets will be reported elsewhere.

As the addition of water into polymer/THF/diamine solution progresses, three processes occur: the change of interfacial energy between different blocks and mixed solvents, the change of the interaction of amine groups with acid groups, and the change of dielectric constant of the solvent mixture. First, since water is a poor solvent for both PS and PMA segments, addition of water into copolymer/THF solution would result in the strengthened association of the PS−PMA blocks. Second, strong repulsions by deprotonated PAA chains would cause expansion of PAA in the corona. Electrostatic repulsions should force PAA chains to take an extended conformation and, consequently, form a larger interfacial curvature toward the hydrophobic blocks in order to alleviate the chain stretching. However, organic multivalent counterions confined in the corona should pose a constraint on the PAA expansion due to their interchain binding. Even so, the PAA corona swelled more and more with an increased amount of water in solution. Finally, electrostatic interactions in the corona, both repulsive interaction between charged PAA chains and the bonding effect of diamine end groups with acidic units of PAA blocks, were diminished by the increase of the dielectric constant of the bulk solvent with water addition (ϵ: 78.5) into THF (ϵ: 7.58). The combined contribution from all the interactions balanced the contact area between hydrophilic and hydrophobic blocks and defined the local interfacial curvature. The dominating effect of water addition was the shrinkage of PS−PMA hydrophobic blocks and expansion of PAA corona, which resulted in micelle structure with increased interfacial curvature. Therefore, varying solvent content provides an additional way to control morphologies in our system. The schematic shown in Figure 5 illustrates the influence of both organic counterions and the ratio of THF to water on assembled structures.

4. Interaction of PAA Chains with Diamines. To better understand diamine−PAA interaction in micelle aggregates, ^{1}H NMR spectroscopy was used to monitor the interaction between diamine and triblock copolymer during the micellization process, while D_2O was added to a solution in deuterated tetrahydrofuran (THF-d_8). Figure 6A shows five typical NMR spectra of PAA_{99}-*b*-PMA_{73}-*b*-PS_{66} in THF-d_8 solution with different amounts of added diamine. The spectra were recorded with stepwise titration of diamine. The peak at 10.8 ppm is due to the resonance of the carboxylic acid proton from PAA, and the two sets of peaks

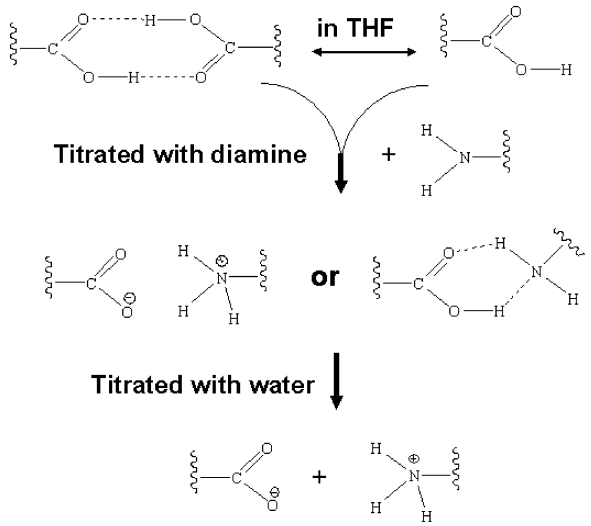

Figure 7. Proposed interaction mechanism between acid groups of PAA segment and amine groups of diamines.

at ca. 7 ppm are ascribed to the aromatic protons from PS. The observed line broadening is typical of polymer due to the low mobility of polymer chain segments and the short relaxation times. When no diamine is present, a very broad NMR resonance exists in the carboxylic acid proton region, suggesting the formation of very large, loosely bound aggregates. The tiny sharp peak in this region is possibly from free acrylic acid ends. With the addition of only 20% equivalency of diamine, the broad carboxylic acid proton resonance was replaced by a sharp peak. This observation could be taken as an indication of complete disruption of preformed large aggregation, although it is also possible that the dramatic line-width change may arise from catalyzed exchange of protons between different carboxyl groups by the small amount added diamine. Further titration of the diamine induced the broadening of the new peak, suggesting the formation and increasing of the size of a second aggregation. It is worth noting that the line width of the two sets of PS proton peaks (around 7 ppm) during the diamine titration process did not change, indicating that the mobility of PS chains was not affected. Monitoring of the micellization process was conducted by further titration with deuterated water. With the progressive addition of water into PAA_{99}-*b*-PMA_{73}-*b*-PS_{66} copolymer/THF solution with constant EDDA concentration (amine:acid = 1:1), the PS proton signals became broadened, weakened significantly, and finally disappeared at 1:2 ratio of THF to water, indicating a gradual decrease of PS chain mobility (Figure 6B). In mixed solvents, the mobility of polymer chains in solution is determined by their local environment. Because water is a nonsolvent for PS, hydrophobic PS segments began to pack more densely and formed micelle cores with the titration of water in order to minimize contact with the increasing water content in a mixed solvent system.

On the basis of these NMR data, a proposed interaction mechanism of amine groups with acid groups is shown in Figure 7. In neat THF solution, the formation of large aggregate structure is due to the hydrogen bonding between carboxylic acid groups. With the progressive titration of diamine, this hydrogen bonding was broken up and replaced with either new hydrogen bonding or compact ionic pairs between amine groups and carboxylic acid groups, causing formation and increasing of the size of a new aggregate. Unfortunately, NMR spectroscopy cannot differentiate exactly whether it is ionic bonding or hydrogen bonding that dominates the binding mechanism. With the addition of water, deprotonation of weak acid PAA by weak

base diamines occurs, and the solvation causes the loose binding of ion pairs. It is highly possible that hydrogen bonding is preferred in a low dielectric constant media, such as THF, and ion pairing in the high dielectric constant media, such as water. In fact, in pure water solution, zeta potential measurements revealed a negatively charged surface for PAA-*b*-PMA-*b*-PS micelles (data not shown), which implies that PAA chains are deprotonated and tend to form ionic pairs with amine groups in pure water solution. Therefore, hydrogen bonds and compact and loose ionic pairs from the amino acid interaction dominated at different stages of the self-assembly process.

Summary

Self-assembled structures originating from a common charged triblock copolymer were tunable via the coassembly of organic, divalent counterions and adjustment of the solvent/nonsolvent conditions. The morphology was strongly dependent on organic counterion chain structure. Hydrophilic diamines promoted morphological changes through interchain binding in the corona. The extent of corona chain crowding due to diamine binding, and consequent micelle geometry manipulation, was dictated by the hydrophilic spacer length; the shortest linkers produced the highest PAA crowding and flat, disk micelles, while longer linkers induced the formation of micelle structure having higher interfacial curvature, i.e., cylinders and spheres. Short, hydrophobic diamines showed a similar interfacial corona effect as observed with hydrophilic linkers. However, diamines with hydrophobic spacer length longer than six methylene units demonstrated the reverse effect and decreased interfacial curvature. It is hypothesized that diamines with the longest hydrophobic spacers interacted with the hydrophobic micelle cores by forming a hairpin structure through which hydrophobic spacers could be placed into the PMA−PS core while the two amine end groups remained in the corona.

These findings offer new opportunities for designing soft materials with controlled morphological complexity on the nanometer scale. Usage of charged block copolymers and organic counterions provides a facile method to modify interfacial curvature. In combination with the solvent selectivity and variation of the concentration of added polyamines, various micellar nanostructure morphologies can be targeted and accessed from a single block copolymer precursor. This simple addition of a series of counterions to affect dramatic morphological changes increases substantially the phase space, which we continue to explore further.

Acknowledgment. We thank Dr. André d'Avignon for assistance and inspired discussion in performing NMR experiments. This material is based upon work supported by the National Science Foundation, Nanoscale Interdisciplinary Research Teams program under Grant DMR-0210247. We also acknowledge the W. M. Keck College of Engineering electron microscopy laboratory at the University of Delaware.

References and Notes

(1) Hawker, C. J.; Russell, T. P. *MRS Bull.* **2005**, *30*, 952−966.
(2) Antonietti, M.; Forster, S. *Adv. Mater.* **2003**, *15*, 1323−1333.
(3) Forster, S.; Konrad, M. *J. Mater. Chem.* **2003**, *13*, 2671−2688.
(4) Park, M.; Harrison, C.; Chaikin, P. M.; Register, R. A.; Adamson, D. H. *Science* **1997**, *276*, 1401−1404.
(5) Stupp, S. I.; LeBonheur, V.; Walker, K.; Li, L. S.; Huggins, K. E.; Keser, M.; Amstutz, A. *Science* **1997**, *276*, 384−389.
(6) Collier, J. H.; Messersmith, P. B. *Annu. Rev. Mater. Res.* **2001**, *31*, 237−263.
(7) Silva, G. A.; Czeisler, C.; Niece, K. L.; Beniash, E.; Harrington, D. A.; Kessler, J. A.; Stupp, S. I. *Science* **2004**, *303*, 1352−1355.
(8) Savic, R.; Luo, L. B.; Eisenberg, A.; Maysinger, D. *Science* **2003**, *300*, 615−618.
(9) Torchilin, V. P. *Nat. Rev. Drug Discov.* **2005**, *4*, 145−160.
(10) Israelachvili, J. N. *Intermolecular & Surface Forces*, 2nd ed.; Academic Press: New York, 1991.
(11) Svenson, S. *Curr. Opin. Colloid Interface Sci.* **2004**, *9*, 201−212.
(12) Lodge, T. P. *Macromol. Chem. Phys.* **2003**, *204*, 265−273.
(13) Discher, B. M.; Won, Y. Y.; Ege, D. S.; Lee, J. C. M.; Bates, F. S.; Discher, D. E.; Hammer, D. A. *Science* **1999**, *284*, 1143−1146.
(14) Pochan, D. J.; Chen, Z. Y.; Cui, H. G.; Hales, K.; Qi, K.; Wooley, K. L. *Science* **2004**, *306*, 94−97.
(15) Cornelissen, J.; Fischer, M.; Sommerdijk, N.; Nolte, R. J. M. *Science* **1998**, *280*, 1427−1430.
(16) Raez, J.; Manners, I.; Winnik, M. A. *J. Am. Chem. Soc.* **2002**, *124*, 10381−10395.
(17) Lodge, T. P.; Hillmyer, M. A.; Zhou, Z. L.; Talmon, Y. *Macromolecules* **2004**, *37*, 6680−6682.
(18) Li, Z. B.; Chen, Z. Y.; Cui, H. G.; Hales, K.; Qi, K.; Wooley, K. L.; Pochan, D. J. *Langmuir* **2005**, *21*, 7533−7539.
(19) Zhang, L. F.; Bartels, C.; Yu, Y. S.; Shen, H. W.; Eisenberg, A. *Phys. Rev. Lett.* **1997**, *79*, 5034−5037.
(20) Zheng, R. H.; Liu, G. J.; Yan, X. H. *J. Am. Chem. Soc.* **2005**, *127*, 15358−15359.
(21) Lodge, T. P.; Bang, J. A.; Li, Z. B.; Hillmyer, M. A.; Talmon, Y. *Faraday Discuss.* **2005**, *128*, 1−12.
(22) Chen, Z. Y.; Cui, H. G.; Hales, K.; Li, Z. B.; Qi, K.; Pochan, D. J.; Wooley, K. L. *J. Am. Chem. Soc.* **2005**, *127*, 8592−8593.
(23) Li, Z. B.; Kesselman, E.; Talmon, Y.; Hillmyer, M. A.; Lodge, T. P. *Science* **2004**, *306*, 98−101.
(24) Jain, S.; Bates, F. S. *Science* **2003**, *300*, 460−464.
(25) Zhang, L. F.; Eisenberg, A. *Science* **1995**, *268*, 1728−1731.
(26) Yan, X. H.; Liu, G. J.; Li, Z. *J. Am. Chem. Soc.* **2004**, *126*, 10059−10066.
(27) Hanley, K. J.; Lodge, T. P.; Huang, C. I. *Macromolecules* **2000**, *33*, 5918−5931.
(28) Quintana, J. R.; Janez, M. D.; Villacampa, M.; Katime, I. *Macromolecules* **1995**, *28*, 4139−4143.
(29) Yu, Y. S.; Zhang, L. F.; Eisenberg, A. *Macromolecules* **1998**, *31*, 1144−1154.
(30) Yu, Y. S.; Eisenberg, A. *J. Am. Chem. Soc.* **1997**, *119*, 8383−8384.
(31) Choucair, A.; Lavigueur, C.; Eisenberg, A. *Langmuir* **2004**, *20*, 3894−3900.
(32) He, Y. Y.; Li, Z. B.; Simone, P.; Lodge, T. P. *J. Am. Chem. Soc.* **2006**, *128*, 2745−2750.
(33) Korczagin, I.; Hempenius, M. A.; Fokkink, R. G.; Stuart, M. A. C.; Al-Hussein, M.; Bomans, P. H. H.; Frederik, P. M.; Vancso, G. J. *Macromolecules* **2006**, *39*, 2306−2315.
(34) Zhang, L. F.; Yu, K.; Eisenberg, A. *Science* **1996**, *272*, 1777−1779.
(35) Lee, A. S.; Butun, V.; Vamvakaki, M.; Armes, S. P.; Pople, J. A.; Gast, A. P. *Macromolecules* **2002**, *35*, 8540−8551.
(36) Forster, S.; Hermsdorf, N.; Leube, W.; Schnablegger, H.; Regenbrecht, M.; Akari, S.; Lindner, P.; Bottcher, C. *J. Phys. Chem. B* **1999**, *103*, 6657−6668.
(37) Li, Y.; Xu, R.; Couderc, S.; Bloor, D. M.; Wyn-Jones, E.; Holzwarth, J. F. *Langmuir* **2001**, *17*, 183−188.
(38) Bronstein, L. M.; Chernyshov, D. M.; Timofeeva, G. I.; Dubrovina, L. V.; Valetsky, P. M.; Obolonkova, E. S.; Khokhlov, A. R. *Langmuir* **2000**, *16*, 3626−3632.
(39) Bronstein, L. M.; Chernyshov, D. M.; Timofeeva, G. I.; Dubrovina, L. V.; Valetsky, P. M.; Khokhlov, A. R. *J. Colloid Interface Sci.* **2000**, *230*, 140−149.
(40) Zhang, K. W.; Lindman, B.; Coppola, L. *Langmuir* **1995**, *11*, 538−542.
(41) Hecht, E.; Hoffmann, H. *Langmuir* **1994**, *10*, 86−91.
(42) Almgren, M.; Vanstam, J.; Lindblad, C.; Li, P. Y.; Stilbs, P.; Bahadur, P. *J. Phys. Chem.* **1991**, *95*, 5677−5684.
(43) Zheng, Y.; Davis, H. T. *Langmuir* **2000**, *16*, 6453−6459.
(44) Bronich, T. K.; Popov, A. M.; Eisenberg, A.; Kabanov, V. A.; Kabanov, A. V. *Langmuir* **2000**, *16*, 481−489.
(45) Kabanov, A. V.; Bronich, T. K.; Kabanov, V. A.; Yu, K.; Eisenberg, A. *J. Am. Chem. Soc.* **1998**, *120*, 9941−9942.
(46) Gohy, J. F.; Varshney, S. K.; Jerome, R. *Macromolecules* **2001**, *34*, 2745−2747.
(47) Gohy, J. F.; Varshney, S. K.; Antoun, S.; Jerome, R. *Macromolecules* **2000**, *33*, 9298−9305.
(48) Khanal, A.; Li, Y.; Takisawa, N.; Kawasaki, N.; Oishi, Y.; Nakashima, K. *Langmuir* **2004**, *20*, 4809−4812.
(49) van der Maarel, J. R. C.; Groenewegen, W.; Egelhaaf, S. U.; Laap, A. *Langmuir* **2000**, *16*, 7510−7519.
(50) Groenewegen, W.; Lapp, A.; Egelhaaf, S. U.; van der Maarel, J. R. C. *Macromolecules* **2000**, *33*, 4080−4086.
(51) Groenewegen, W.; Egelhaaf, S. U.; Lapp, A.; van der Maarel, J. R. C. *Macromolecules* **2000**, *33*, 3283−3293.

(52) Dingenouts, N.; Patel, M.; Rosenfeldt, S.; Pontoni, D.; Narayanan, T.; Ballauff, M. *Macromolecules* **2004**, *37*, 8152−8159.
(53) Zhang, L. F.; Eisenberg, A. *Macromolecules* **1996**, *29*, 8805−8815.
(54) Ma, Q. G.; Wooley, K. L. *J. Polym. Sci., Part A: Polym. Chem.* **2000**, *38*, 4805−4820.
(55) Lapouyade, R.; Morand, J. P. *J. Chem. Soc., Chem. Commun.* **1987**, 223−224.
(56) Ciuffarin, E.; Isola, M.; Leoni, P. *J. Org. Chem.* **1981**, *46*, 3064−3070.
(57) Halperin, A.; Tirrell, M.; Lodge, T. P. *Adv. Polym. Sci.* **1992**, *100*, 31−71.
(58) Zhulina, E. In *Solvents and Self-Organization of Polymers*; Webber, S. E., Zdemek Tuzar, P. M., Eds.; Kluwer Academic Publishers: Dordrecht, 1995; pp 227−258.
(59) Bloomfield, V. A. *Biopolymers* **1997**, *44*, 269−282.
(60) Plum, G. E.; Arscott, P. G.; Bloomfield, V. A. *Biopolymers* **1990**, *30*, 631−643.
(61) Schellman, J. A.; Parthasarathy, N. *J. Mol. Biol.* **1984**, *175*, 313−329.
(62) Lu, Z. H.; Liu, G. J.; Liu, F. T. *Macromolecules* **2001**, *34*, 8814−8817.

MA0609026